Decoding of Calcium Oscillations by Phosphorylation Cycles: Analytic Results

Carlos Salazar, Antonio Zaccaria Politi, and Thomas Höfer
Research Group Modeling of Biological Systems, German Cancer Research Center, Heidelberg, Germany

ABSTRACT Experimental studies have demonstrated that Ca^{2+}-regulated proteins are sensitive to the frequency of Ca^{2+} oscillations, and several mathematical models for specific proteins have provided insight into the mechanisms involved. Because of the large number of Ca^{2+}-regulated proteins in signal transduction, metabolism and gene expression, it is desirable to establish in general terms which molecular properties shape the response to oscillatory Ca^{2+} signals. Here we address this question by analyzing in detail a model of a prototypical Ca^{2+}-decoding module, consisting of a target protein whose activity is controlled by a Ca^{2+}-activated kinase and the counteracting phosphatase. We show that this module can decode the frequency of Ca^{2+} oscillations, at constant average Ca^{2+} signal, provided that the Ca^{2+} spikes are narrow and the oscillation frequency is sufficiently low—of the order of the phosphatase rate constant or below. Moreover, Ca^{2+} oscillations activate the target more efficiently than a constant signal when Ca^{2+} is bound cooperatively and with low affinity. Thus, the rate constants and the Ca^{2+} affinities of the target-modifying enzymes can be tuned in such a way that the module responds optimally to Ca^{2+} spikes of a certain amplitude and frequency. Frequency sensitivity is further enhanced when the limited duration of the external stimulus driving Ca^{2+} signaling is accounted for. Thus, our study identifies molecular parameters that may be involved in establishing the specificity of cellular responses downstream of Ca^{2+} oscillations.

INTRODUCTION

Cell signaling induced by extracellular stimuli is often accompanied by an increase in the cytosolic calcium concentration $[Ca^{2+}]_c$ that, ultimately, regulates a plethora of cellular processes, including secretion, contraction, learning, and proliferation (1–4). Such regulation is mediated by Ca^{2+}-dependent enzymes that, in turn, modify downstream targets commonly by phosphorylation. In many cell types, changes in $[Ca^{2+}]_c$ occur as repetitive spikes that increase their frequency with the strength of the stimulus (5,6). Information can also be encoded in the amplitude of Ca^{2+} oscillations, which may change with the extracellular stimulus (7–9) and may also depend on the subcellular localization of the target (10,11). Understanding how an extracellular stimulus, encoded in the frequency and amplitude of Ca^{2+} oscillations, is interpreted by different physiological processes is one of the major challenges in the study of Ca^{2+} signaling.

Various experiments have suggested that Ca^{2+} oscillations may be advantageous compared to a constant rise in $[Ca^{2+}]_c$ because they increase the efficiency of gene expression at low levels of stimulation (12,13). A long-standing question is how a ubiquitous messenger like Ca^{2+} achieves specificity in its action. Recent data indicate the ability of calmodulin and protein kinase C (PKC) to decode the amplitude of Ca^{2+} oscillatory signal into an appropriate cellular response (14,15). It has been shown that the sensitivity to Ca^{2+} oscillations of different transcription factors such as the nuclear factor of activated T cells (NFAT), nuclear factor kappa B (NFκB) (12,13,16), Ca^{2+}-dependent enzymes such as calmodulin (CaM) kinase II (17), and mitochondria (18,19), can depend on the oscillation frequency. Moreover, when the stimulus is transient, the effect of Ca^{2+} oscillations can be maximized within a certain range of frequencies (13,16,20). In Ca^{2+} oscillations, higher frequency implies a higher density of practically uniformly shaped Ca^{2+} spikes and thus also a higher average $[Ca^{2+}]_c$. Thus, the question arises whether the observed increases in target response with rising oscillation frequency are simply due to an increase in the average Ca^{2+} signal or present a true frequency decoding.

Previous theoretical work has focused on how frequency-encoded information is processed by Ca^{2+}-regulated proteins (21–23). Frequency decoding is characterized by higher average levels of phosphorylated protein when the frequency of Ca^{2+} oscillations is increased. Detailed models of protein phosphorylation driven by regular Ca^{2+} oscillations have been developed for CaM kinase II (14,24,25), glycogen phosphorylase (26,27), and mitogen-activated protein kinase cascades (28,29). Decoding of Ca^{2+} signals more complex than periodic spiking (e.g., bursting oscillations) has been recently theoretically explored (30,31). Numerical simulations have shown that Ca^{2+} oscillations can be more efficient for protein phosphorylation compared to constant Ca^{2+} signals of equal average $[Ca^{2+}]_c$. The nonlinear dependence of protein activation on Ca^{2+} stimulation, arising from diverse mechanisms, such as cooperative Ca^{2+} binding or zero-order

Submitted July 24, 2007, and accepted for publication September 26, 2007.

Carlos Salazar and Antonio Zaccaria Politi contributed equally to this work.

Address reprint requests to Carlos Salazar, E-mail: c.salazar@dkfz-heidelberg.de; or Thomas Höfer, E-mail: t.hoefer@dkfz-heidelberg.de.

Antonio Politi's present address is the Dept. of Mathematics, University of Auckland, 38 Princes St., Auckland, New Zealand.

Editor: Ian Parker.

0006-3495/08/02/1203/13 $2.00

doi: 10.1529/biophysj.107.113084

ultrasensitivity, turns out to be of major importance for an efficient processing of oscillatory signals. Furthermore, these models predict that the Ca^{2+} oscillation frequency can discriminate among different signaling pathways.

Although these theoretical studies have provided insight into the mechanisms involved in calcium decoding, their conclusions are based on numerical simulations of detailed models for specific proteins (reviewed in (32)). Because of the large numbers of Ca^{2+}-regulated proteins in signal transduction and gene transcription, it is desirable to establish in general terms which molecular properties shape the response to Ca^{2+} oscillations. Investigating Ca^{2+} decoding in an analytically tractable model may provide more insight into the following issues:

- How sensitively can a target protein respond to changes in the frequency of calcium oscillations?
- Under which conditions are Ca^{2+} oscillations more potent than a constant signal in activating a target protein?
- Which properties determine the existence of an optimal activating signal for a particular target?
- Under which conditions can target proteins be differentially activated by Ca^{2+} signals?

Some challenges for such analysis are the nonstationarity of the Ca^{2+} signal and the nonlinearity of the Ca^{2+} dependent processes. The description of Ca^{2+} oscillations using a piecewise constant function can facilitate an analytical solution of the kinetic equations (31,33,34). Indeed, such square-shaped pulses have been used in several experiments (12,13,17) and for numerical simulations (20,35).

In this article, we attempt to establish in general terms which molecular properties determine the target response to oscillatory Ca^{2+} signals. To this aim, we employed an analytically tractable model of a prototypical Ca^{2+}-decoding module, consisting of a target protein controlled by a Ca^{2+}-activated kinase and the counteracting phosphatase. The modeling of Ca^{2+} oscillations by square-shaped pulses allowed the derivation of a general formula for the target activity as a function of three dimensionless parameters.

Using this formula, we first asked whether a true frequency decoding, at constant average Ca^{2+} signal, is possible. We then examined the conditions under which oscillatory signals are more potent in activating the target protein than constant signals with the same average calcium. To assess the kinetics of the target, we defined an activation time that quantifies the time necessary to reach the maximal target activity. The expressions for the activation time and target activity were used to analyze signaling specificity. In particular, we investigated which molecular parameters determine the optimal signal shape for a limited amount of calcium. Collectively, our results demonstrate that the nonlinear activation of a protein by a Ca^{2+}-dependent kinase represents a core system for decoding Ca^{2+} oscillations, and rationalize why oscillatory stimuli increase the efficiency and specificity of cell signaling.

MATHEMATICAL MODEL

We consider an activation-inactivation cycle of a target protein X (Fig. 1 *A*). Its activation is induced by phosphorylation through a Ca^{2+}-dependent kinase Y, and it is inactivated by dephosphorylation. Cooperative activation of the kinase by Ca^{2+}, as observed, for example, for Ca^{2+}/CaM-dependent kinases (36,37), is described by the binding of n ions of Ca^{2+}. The fractions of active kinase Y and phosphorylated (active) target protein X obey, in the simplest model,

$$\frac{dY}{dt} = \alpha_Y S(t)^n (1 - Y) - \beta_Y Y, \tag{1}$$

$$\frac{dX}{dt} = \alpha_X Y_T Y (1 - X) - \beta_X X, \tag{2}$$

where Y_T represents the total concentration of kinase, $S(t)$ describes the time course of the Ca^{2+} signal, α_Y and β_Y are the rate constants of Ca^{2+} binding and release, and the rate constants of phosphorylation and dephosphorylation are denoted by α_X and β_X, respectively.

In many cases, Ca^{2+} binding will be much faster than (de)phosphorylation reactions, so that we can assume the binding equilibrium, $dY/dt \approx 0$. Equation 2 then becomes

$$\frac{dX}{dt} = \alpha(S) - (\alpha(S) + \beta)X, \tag{3}$$

where, for simplicity, $\beta = \beta_X$. Between calcium spikes, the kinase activity is negligible so that the response time of the target protein is β^{-1}.

The dependence of the phosphorylation rate constant on Ca^{2+} concentration takes the form of the Hill equation

$$\alpha(S) = \hat{\alpha} \frac{(S/K_S)^n}{(S/K_S)^n + 1}, \tag{4}$$

with the maximal value $\hat{\alpha} = \alpha_X Y_T$, the half-saturation constant $K_S = \sqrt[n]{\beta_Y/\alpha_Y}$, and the Hill-coefficient n. Hill equations provide good fits for more realistic Ca^{2+} binding mechanisms, in which case n can take noninteger values (20,30).

Cytosolic Ca^{2+} oscillations consist of a series of spikes separated by intervals of resting Ca^{2+} concentration (38). To enable analytic treatments, Ca^{2+} oscillations are described by a piecewise constant function

$$S(t) = \begin{cases} S_0, & iT \le t < iT + \Delta \\ 0, & iT + \Delta < t < (i+1)T \end{cases}$$
$$i = 0, \ldots, \infty, \tag{5}$$

characterized by period T, amplitude S_0, and spike width Δ (Fig. 1 *B*). For simplicity, the basal Ca^{2+} concentration has been set to zero.

RESULTS

The mean activity of the target protein depends on three dimensionless parameters

Let us assume that before the onset of calcium oscillations, the target protein is completely inactive (i.e., unphosphorylated).

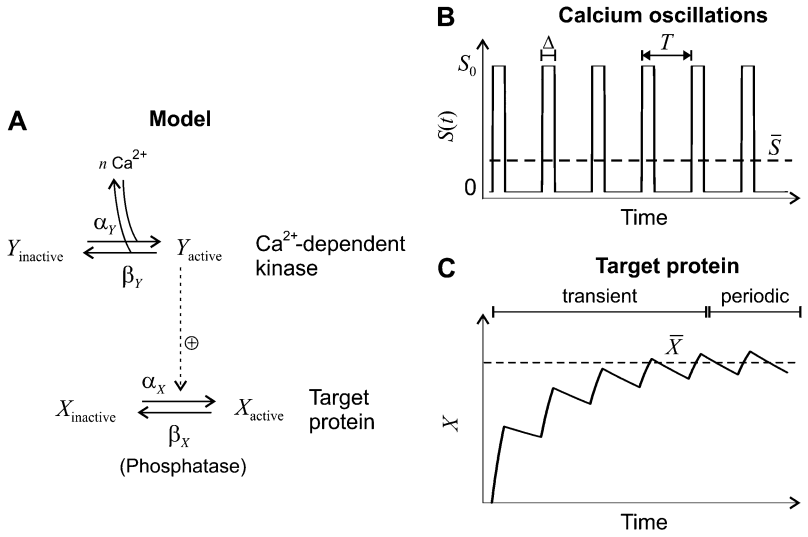

FIGURE 1 Model for the decoding of Ca^{2+} oscillations by a target protein. (*A*) Model scheme. (*B*) Oscillations in the Ca^{2+} concentration $S(t)$ have period T, amplitude S_0, spike width Δ, and average $\bar{S}$. (*C*) The calcium signal induces oscillations in the phosphorylated (active) target protein. After an initial transient, the time-average target activity reaches the steady value $\bar{X}$.

The target's response to the oscillations goes through an initial transient to reach an (approximately) periodic state (Fig. 1 *C*). The mean target activity $\bar{X}_\mathrm{i}$ during the i^{th} oscillation cycle is

$$\bar{X}_\mathrm{i} = \frac{1}{T}\int_{\mathrm{iT}}^{(\mathrm{i}+1)\mathrm{T}} X(t)dt. \tag{6}$$

The average is a good measure of the target protein's response if the amplitude of the protein activity oscillations is not too large, that is, when the system integrates the oscillations. This has been seen in the responses of gene expression rates and of mitochondrial metabolism to calcium oscillations (12,16,18,19). However, even if the target amplitudes were large, the average is a useful diagnostic of how sensitively the system responds to the oscillatory signal.

The approximation for the Ca^{2+} spikes (see Eq. 5) allows the derivation of an analytic expression for the average $\bar{X}_\mathrm{i}$. After some algebra, one finds for its stationary value $\bar{X} = \lim_{\mathrm{i}\to\infty} \bar{X}_\mathrm{i}$ (see Appendix A):

$$\bar{X} = X_{\max}\left[\gamma + \frac{\omega\sigma}{1+\sigma}\frac{(1-e^{-\gamma(1+\sigma)/\omega})(1-e^{-(1-\gamma)/\omega})}{1-e^{-(1+\gamma\sigma)/\omega}}\right]. \tag{7}$$

This equation shows how the original parameters combine into three dimensionless parameters that govern the response of the system, as follows here.

The effective activation rate σ during the calcium spike

$$\sigma = \frac{\hat{\alpha}}{\beta}\frac{(S_0/K_\mathrm{S})^\mathrm{n}}{1+(S_0/K_\mathrm{S})^\mathrm{n}}, \tag{8}$$

measures how the calcium amplitude S_0 is sensed by the kinase with respect to binding affinity ($1/K_\mathrm{S}$) and cooperativity of kinase activation (Hill coefficient n), and how fast phosphorylation of the target is compared to its dephosphorylation ($\hat{\alpha}/\beta$).

The relative oscillation frequency ω,

$$\omega = \frac{1}{\beta T}, \tag{9}$$

expresses how fast the oscillations are compared with the basal response time of the protein β^{-1} (see Eq. 3). Thus, the parameter combines the two timescales in the problem. Large ω means fast calcium oscillations and/or a slow response time of the phosphorylation cycle, in which case the phosphorylation cycle will integrate over the oscillations and the amplitude of the oscillations in target activity is small. Conversely, if ω is small, the target activity will closely follow each cycle of the calcium oscillations.

The duty ratio of the oscillations γ,

$$\gamma = \frac{\Delta}{T}, \tag{10}$$

gives the part of the oscillation period during which calcium is elevated and the kinase is active. Hence, the average calcium concentration in the oscillations is

$$\bar{S} = \gamma S_0. \tag{11}$$

The maximal activity of the target protein $X_{\max}$ is a function of σ,

$$X_{\max} = \frac{\sigma}{1+\sigma}. \tag{12}$$

Target activity is sensitive to the frequency of narrow calcium spikes

It turns out that the mean target activity $\bar{X}$ is a monotonically increasing function of all three parameters on their natural intervals $\sigma \in [0,\infty)$, $\omega \in [0,\infty)$, and $\gamma \in [0,1)$. Increases in the activation rate, oscillation frequency, or duty ratio would therefore all raise the target activity. As experiments on many cell types show that the dose of the external stimuli (e.g.,

hormones and local mediators) controls primarily the frequency of calcium oscillations and leaves the amplitude unchanged, we asked how sensitively the target protein can respond to variations in frequency. In the limit of slow oscillations (or a rapidly responding protein), we obtained the target activity as

$$\bar{X}(\omega\to 0) = \gamma X_{\max} = \frac{\sigma\gamma}{1+\sigma}. \tag{13}$$

For fast oscillations (or a slowly responding protein), we found

$$\bar{X}(\omega\to\infty) = \frac{(1+\sigma)\gamma}{1+\sigma\gamma}X_{\max} = \frac{\sigma\gamma}{1+\sigma\gamma}. \tag{14}$$

The frequency sensitivity of the target's response to calcium oscillations with constant amplitude becomes maximal,

$$\underset{\gamma}{\text{maximize}}[\bar{X}(\omega\to\infty) - \bar{X}(\omega\to 0)], \tag{15a}$$

$$\sigma = \text{const.}, \tag{15b}$$

when the duty ratio obeys

$$\gamma_{\text{opt}} = \frac{\sqrt{1+\sigma}-1}{\sigma}. \tag{16}$$

The optimal duty ratio γ_{opt} lies between 0.5 (for $\sigma = 0$) and 0 (for $\sigma \to \infty$). Hence, calcium oscillations whose frequency can efficiently drive changes in target activity have duty ratios below 0.5, i.e., the spikes occupy less than half of the oscillation. Interestingly, the observed calcium oscillations, for example in liver cells, have duty ratios between 0.05 and 0.5 (39).

Importantly, when activation rate σ and duty ratio γ are constant and only the relative oscillation frequency ω is varied, the average calcium concentration $\bar{S}$ remains constant (Fig. 2 *A*). Therefore, the system can respond purely to changes in the frequency of the calcium signal if the calcium spikes are sufficiently narrow compared to the period of the oscillations. An example of this true frequency decoding is shown in Fig. 2 *B*. Note that the asymptotic value $\bar{X}(\omega\to\infty)$ is practically reached already for $\omega \geq 1$. This implies that the target protein activity becomes frequency-insensitive when the oscillation period gets in the range of the basal response time of the target protein (see Eq. 9). We have found this to be the typical behavior for a wide range of parameter values.

These results demonstrate that true frequency decoding, at constant average Ca^{2+} signal, can occur provided that the Ca^{2+} spikes are narrow and the oscillation frequency is of the order of the target inactivation rate or below.

Oscillations are more potent than constant signals when the kinase binds calcium cooperatively and with low affinity

Given a certain amount of calcium per unit time, what is the signal shape that best activates the target protein? For the piecewise constant oscillatory signal (Eq. 5), the shape at a given calcium average $\bar{S}$ is uniquely defined by fixing period T and duty ratio γ, where the latter automatically defines the amplitude $S_0 = \bar{S}/\gamma$. Setting the frequency, the optimal signal shape is therefore the solution of

$$\underset{\gamma}{\text{maximize}}\,\bar{X}, \tag{17a}$$

$$\bar{S} = \gamma S_0 = \text{const.} \tag{17b}$$

Using Eq. 14, for high-frequency oscillations, one obtains the maximal target response for

$$\gamma_{\max} = \frac{\bar{S}/K_S}{\sqrt[n]{n-1}}. \tag{18}$$

If calcium activation of the kinase is noncooperative or negatively cooperative, $n \leq 1$, there is no $\gamma_{\max}$. Indeed, for $n \leq 1$, $\bar{X}$ is a monotonically increasing function of γ when the average calcium signal is constrained (Eq. 17b). Therefore, the maximal response will be obtained at $\gamma = 1$ (that is, the constant calcium signal).

However, when calcium activation of the kinase displays positive cooperativity, $n > 1$, $\gamma_{\max}$ can be below 1. Therefore, an oscillatory signal can be more potent in activating the target than a constant signal. The critical case occurs obviously when the maximum is attained for $\gamma = 1$ (constant signal). From Eq. 18, we then found that if the condition

$$K_S > \frac{S_0}{\sqrt[n]{n-1}} \tag{19}$$

holds, the maximum of $\bar{X}$ occurs for $0 < \gamma < 1$, and hence oscillations with the duty ratio given by Eq. 18 activate the target most strongly. In particular, this oscillatory signal

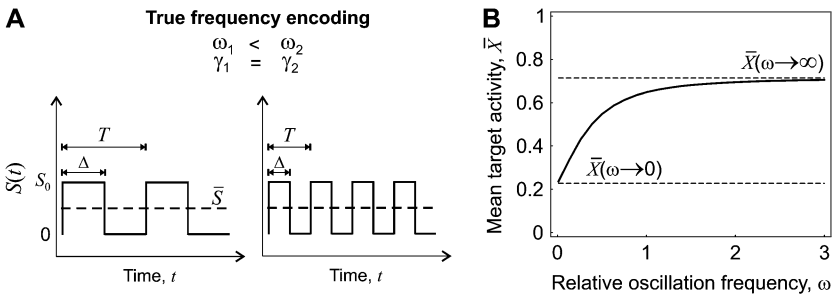

FIGURE 2 Target activity is sensitive to the frequency of narrow calcium spikes. (*A*) True frequency encoding occurs when the relative frequency ω changes while both amplitude S_0 and average $\bar{S}$ stay constant. (*B*) An example of true frequency decoding is shown here. The mean target activity $\bar{X}$ is plotted against ω using Eq. 7. The values of $\bar{X}$ in the limit of very slow and very fast oscillations (Eqs. 13 and 14, respectively) are indicated by dashed lines. Parameters: $\sigma = 10$, $\gamma = 0.25$.

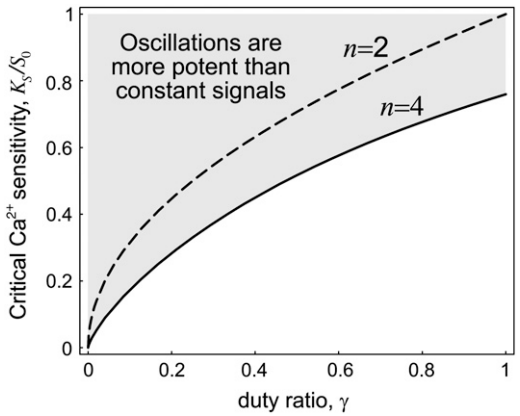

FIGURE 3 Critical Ca^{2+} sensitivity for an efficient decoding by oscillations. The critical Ca^{2+} dissociation constant K_S (relative to the spike amplitude S_0), above which Ca^{2+} oscillations are more potent than a constant Ca^{2+} signal, is plotted as a function of the duty ratio γ. Curves were obtained using Eq. 20. Parameters: $n = 2$ (*dashed line*), $n = 4$ (*solid line*).

is more potent than a constant signal of the same average calcium.

The function $\sqrt[n]{n-1}$ lies between 1 and 1.321 for a cooperative calcium decoder with $2 < n < \infty$ (the maximum is attained at $n = 4.5911$). Therefore, an efficient decoder must have comparatively weak calcium affinity, with dissociation constant K_S lying around the peak concentration of the calcium spike S_0 or above.

Equation 19, for the superiority of oscillations over constant calcium signals, holds for any duty ratio. However, calcium oscillations typically have rather low duty ratios ($\gamma < 0.5$). In this case, the requirement for calcium affinity becomes less stringent. At a given duty ratio γ, oscillations are superior over constant signals if the calcium sensitivity of the kinase, relative to the spike amplitude, satisfies (see Appendix B):

$$\frac{K_S}{S_0} > \sqrt[n]{\frac{\gamma^n - \gamma^{n+1}}{\gamma - \gamma^n}}. \qquad (20)$$

The decrease of the critical dissociation constant with decreasing duty ratio is shown in Fig. 3 for two distinct values of n. So far, all expressions were derived for the case of high-frequency oscillations. We obtained very similar expressions for the general case (Appendix B).

In summary, our theory shows that Ca^{2+} oscillations activate the target of a Ca^{2+}-dependent kinase more efficiently than a constant signal if 1), Ca^{2+} acts cooperatively on the kinase ($n > 1$); and 2), the Ca^{2+} affinity of the kinase is rather low. As an example, we consider typical cytoplasmic Ca^{2+} spikes with $S_0 = 800$ nM and $\gamma = 0.3$, yielding a critical K_S of 300–440 nM for Hill coefficient of 2–4. Indeed, a range of prominent calcium-activated enzymes appears to satisfy the conditions as an efficient oscillation decoder (Table 1).

Target responses to modulations of Ca^{2+} frequency and amplitude

The case of true frequency decoding, in which the shape of Ca^{2+} oscillations is varied but the average Ca^{2+} concentration seen by the protein remains unchanged, has been experimentally studied by means of an engineered control of calcium oscillations. However, in biological reality this case does not seem characteristic. Calcium spikes have a typical width, which is independent of the oscillation period (39). Therefore, an increase in the spike frequency at constant spike amplitude will be accompanied by an increase in the duty ratio γ and hence the average calcium level $\bar{S}$. We have designated this case as biological frequency encoding. Changes in oscillation period T affect ω as well as γ (since $\Delta = const.$) while $\sigma = const.$ (Fig. 4 *A*).

We compared the target activity achieved with constant signals and frequency-encoded oscillatory signals of the same average calcium $\bar{S}$. In the absence of cooperativity in Ca^{2+} binding ($n = 1$), a constant signal (Fig. 4 *B*, *dashed line*) is always more efficient in activating the target protein than an oscillatory signal (*solid lines*). On the contrary, when the kinase is activated cooperatively by Ca^{2+} (shown for

TABLE 1 Examples of calcium-regulated proteins

Protein	Hill coefficient, n	Dissociation constant, K_S	Localization	References
Phospholipase Cδ	2–3	0.4–2 μM	Cytoplasm, plasma membrane	(50,51)
Protein kinase Cβ*	2.3	35 μM	Cytoplasm, plasma membrane	(52)
Calmodulin†	1.8	25 μM	Cytoplasm	(53)
Ca^{2+}/Calmodulin-dependent protein kinase II‡	4.4	1.6–5.8 μM	Dendritic spines	(54)
Calcineurin‡	2.8–3	0.6–1.3 μM	Cytoplasm	(55)
Troponin C§	2.8	4.3 μM	Muscle	(56)
Mitochondrial Ca^{2+} uniporter	2	10–70 μM	Mitochondria	(57)

*Ca^{2+} binding to the C2 domain of PKC was measured in vitro in the absence of phospholipids (52).

†Calmodulin contains four Ca^{2+} binding sites. In vitro experiments by Linse et al. (53) suggest dissociation constants of 20, 0.6, 40, and 5 μM at physiological salt concentrations. The values shown in the table correspond to the effective Hill coefficient and dissociation constant assuming a sequential binding of Ca^{2+} (58).

‡Effective dissociation constant and Hill coefficient for calcineurin bound to calmodulin.

§Troponin C has two low-affinity and two high-affinity Ca^{2+} binding sites. The reported dissociation constants range from 0.2 to 1 μM for the low-affinity sites and from 15.6 to 40 μM for the high-affinity sites (56). The value shown in the table corresponds to the contraction of a reconstituted muscle.

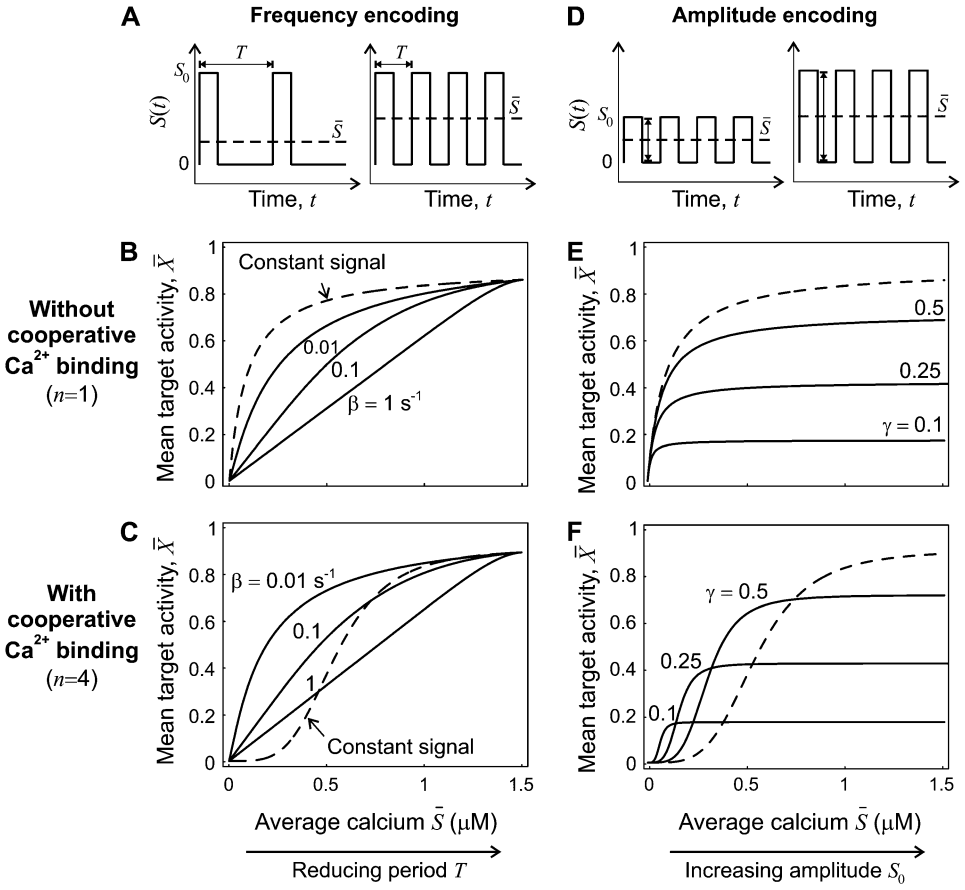

FIGURE 4 Encoding and decoding of Ca^{2+} frequency and amplitude. (*A*) Biological frequency encoding: Oscillation period T changes, and therewith the calcium average $\bar{S}$, while amplitude S_0 remains constant. (*B* and *C*) Frequency decoding: Target activity $\bar{X}$ in response to oscillatory (*solid lines*) or constant (*dashed line*) Ca^{2+} signals. For the oscillatory signal, the average Ca^{2+} concentration $\bar{S}$ is increased by reducing the oscillation period T. (*B* and *C*) Correspond to noncooperative ($n = 1$) and cooperative ($n = 4$) calcium binding, respectively. (*D*) Biological amplitude encoding: Oscillation amplitude S_0 changes, and therewith the calcium average $\bar{S}$, while the period T remains constant. (*E* and *F*) Amplitude decoding: Target activity $\bar{X}$ in response to oscillatory (*solid lines*) or constant (*dashed line*) Ca^{2+} signals. For the oscillatory signal, $\bar{S}$ is changed by increasing the oscillation amplitude S_0. Panels *E* and *F* correspond to noncooperative ($n = 1$) and cooperative ($n = 4$) calcium binding, respectively. Parameters: $\hat{\alpha}/\beta = 10$, $K_S = 1$ μM, $S_0 = 1.5$ μM, $\Delta = 10$ s; in panels *B* and *C*, $\beta = 0.01$, 0.1, 1/s; in panels *E* and *F*, $\beta = 0.1$/s, and $\gamma = 0.1, 0.25, 0.5$.

$n = 4$), the detection of Ca^{2+} oscillations with lower average concentration is considerably enhanced compared to the constant signal (Fig. 4 *C*, *solid* and *dashed lines*, respectively). In particular, targets with slow activation-inactivation cycles are more efficiently activated than rapidly responding targets (compare the *solid lines* in Fig. 4, *B* and *C*).

Differences in spike amplitudes are particularly relevant in the context of subcellular localization of the target, because in restricted spaces such as between the ER and nearby mitochondria the calcium amplitude can be much higher than in the bulk cytoplasm. Thus, we have defined this second strategy to activate the target protein as biological amplitude encoding. The calcium amplitude S_0 (and hence σ) varies, while $\omega = const.$, $\gamma = const$. This has the consequence that average calcium $\bar{S} = \gamma S_0$ also varies (Fig. 4 *D*). In the absence of cooperativity ($n = 1$), as for frequency encoding, a constant signal (Fig. 4 *E*, *dashed line*) is more efficient in activating the target protein than an oscillatory signal (*solid lines*). In the presence of cooperativity ($n = 4$, Fig. 4 *F*), oscillations enhance signaling efficiency by shifting the activation threshold of the target protein to weaker Ca^{2+} stimuli (lower values of $\bar{S}$). However, the maximal value of the mean target activity $\bar{X}$ is then also reduced.

Thus, at low levels of stimulation, Ca^{2+} oscillations can be more potent in activating a target than constant signals of the same average calcium irrespective of whether the information is transmitted by the amplitude or by the frequency of oscillations. However, this requires cooperativity in the calcium binding.

Calcium oscillations increase the specificity of target activation by sensing its response kinetics

So far, we have examined the activation of a single target protein. A long-standing question is how a ubiquitous messenger like Ca^{2+}, with a large number of downstream targets, can elicit selective responses. Experiments suggest that such specificity may arise from differences in Ca^{2+} sensitivity and response kinetics among the downstream targets. Therefore, we compared a slow, insensitive phosphorylation cycle 1 with a fast, sensitive cycle 2 ($\beta_1 < \beta_2$, $K_{S1} > K_{S2}$).

When the Ca^{2+} concentration remains constant, the more sensitive protein 2 will be preferentially activated (Fig. 5 *A*). If both phosphorylation cycles differ only in their response kinetics, their target proteins would be equally activated. The question arises whether oscillations can sense the response kinetics of phosphorylation cycles and so increase target specificity compared to a constant signal. Can oscillatory signals upregulate one target protein and downregulate another and vice versa? We demonstrated above that, at a given

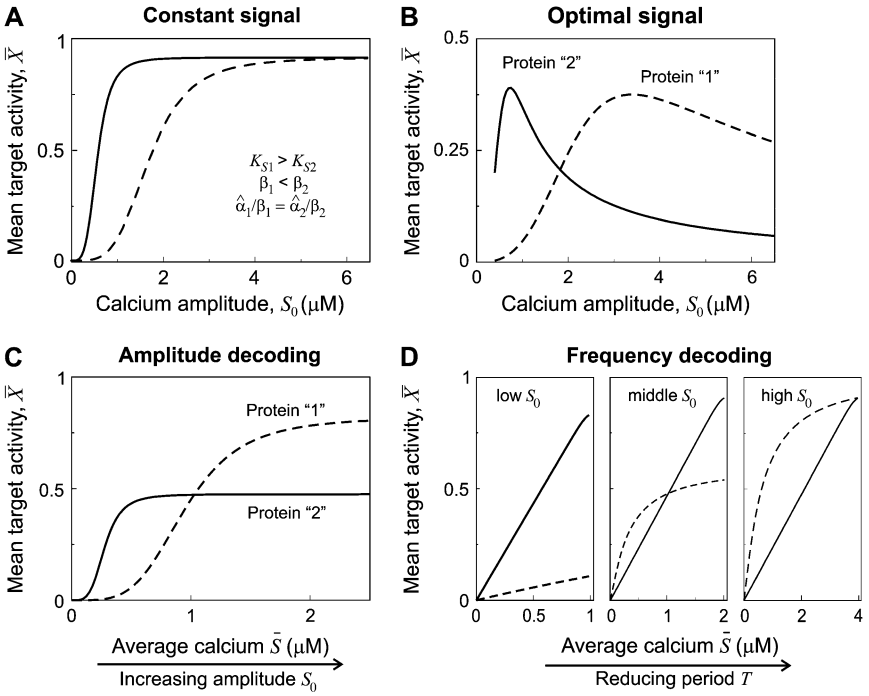

FIGURE 5 Specificity of target activation. Protein 1 is less Ca^{2+}-sensitive and responds slower than protein 2. (*A*) A constant Ca^{2+} signal preferentially activates protein 2. (*B*) When the average is kept constant, an optimal oscillatory signal exists for each target protein. (*C*) Amplitude-encoded oscillatory signals activate primarily protein 2 at low amplitudes and protein 1 at high amplitudes. (*D*) Frequency-encoded signals preferentially activate protein 2 at low amplitudes and protein 1 at high amplitudes, irrespective of the oscillation period. Protein parameters: $\hat{\alpha}_1 = 0.1/\mathrm{s}, \beta 1 = 0.01/\mathrm{s}, \hat{\alpha}_2 = 10/\mathrm{s}, \beta_2 = 1/\mathrm{s}, n_1 = n_2 = 4, K_{S1} = 3\,\mu\mathrm{M}, K_{S2} = 1\,\mu\mathrm{M}.Ca^{2+}$ signal parameters: Spike width $\Delta = 20$ s; in panel *C*, $\gamma = 0.5$; in panel *D*, $S_0 = 1{,}2{,}4\ \mu$M.

calcium average, a maximal target activity is obtained for an oscillatory signal of amplitude $S_0 = K_S \sqrt[n]{(n-1)/(\hat{\alpha}/\beta + 1)}$ (see Appendix B). This optimal amplitude depends not only on Ca^{2+} sensitivity but also on the response kinetics of the cycle. The activities of proteins 1 and 2 become maximal at distinct signal amplitudes and thus they are selectively activated by Ca^{2+} oscillations (Fig. 5 *B*).

In the case of amplitude-encoded signals, protein 2 prevails at low levels of stimulation due to its stronger Ca^{2+} sensitivity, whereas the slowly responding protein 1 predominates at higher Ca^{2+} concentrations (Fig. 5 *C*). On the other hand, frequency encoding provides three different scenarios, depending on the oscillation amplitude. At sufficiently low or sufficiently high amplitudes, one of the two proteins prevails irrespective of the oscillation period. For middle amplitudes, however, protein 1 and protein 2 will be preferentially activated at low and high oscillation frequencies, respectively (Fig. 5 *D*). Thus, Ca^{2+} oscillations ensure a more specific regulation of target proteins because they can also sense the response kinetics of phosphorylation cycles.

Phosphorylation cycle integrates Ca^{2+} oscillations when their frequency is larger than the target inactivation rate

Phosphorylation cycles can either closely follow each cycle of the Ca^{2+} oscillations or rather integrate over the oscillations. The phosphorylation cycle integrates the Ca^{2+} signal if the target activity continuously increases after each Ca^{2+} oscillation. To investigate under which conditions a phosphorylation cycle behaves as an integrator of Ca^{2+} oscillations, we need to evaluate how fast the target protein responds to the Ca^{2+} stimulus. Therefore, we defined the characteristic time τ (see Fig. 6 *A*)

$$\tau = \frac{Q}{\bar{X}}, \quad \text{with} \quad Q = T\sum_{i=0}^{\infty} \bar{X} - \bar{X}_i, \tag{21}$$

which describes the mean time needed to attain the stationary target activity $\bar{X}$ in response to an oscillatory signal. Equation 21 resembles the characteristic time previously defined for a constant signal (40). A general expression for τ has been derived in Appendix A (Eq. 35). For fast oscillations, or a slowly responding protein, one obtains

$$\frac{\tau}{T} \approx \frac{\omega}{1+\sigma\gamma} - \frac{1-\gamma}{2}. \tag{22}$$

As shown in Fig. 6 *B*, for a large range of periods, Eq. 22 (*dashed lines*) is a good approximation of the exact solution (*solid lines*). The ratio τ/T gives the mean number of Ca^{2+} spikes needed to attain the stationary activity $\bar{X}$, and thus is a measure of whether the phosphorylation cycles integrates over the oscillations. When $\tau/T < 1$, the stationary activity $\bar{X}$ will be reached during the first oscillation; this is always the case when $\omega = 1/\beta T < 1$. Thus, when the oscillation period is larger than the characteristic time $1/\beta$ of target inactivation, the Ca^{2+} signal is not integrated by the system. Moreover, large signal amplitudes (large σ) can also reduce the number of spikes necessary to attain $\bar{X}$. Together, our results show that phosphorylation cycles integrate Ca^{2+} oscillations if their amplitude is low and their frequency is larger than the inactivation rate of the target.

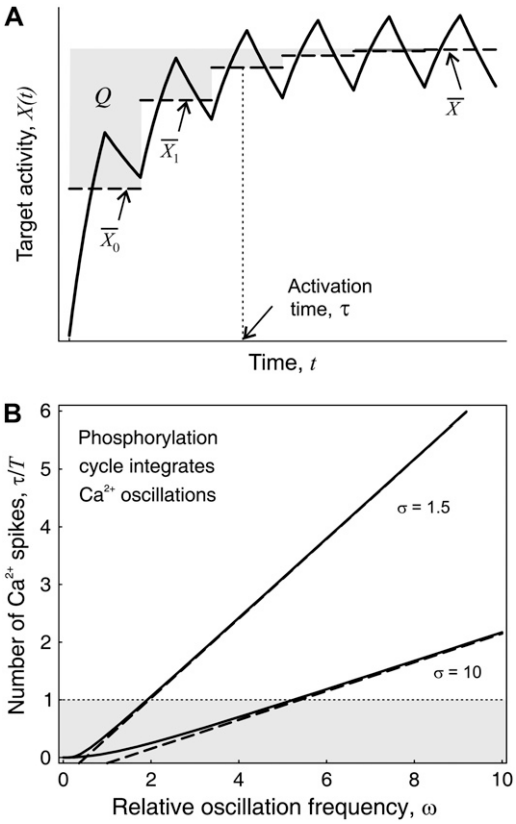

FIGURE 6 Kinetics of target activation by Ca^{2+} oscillations. (*A*) Shown is the time course of the active target X in response to an oscillatory signal (*solid line*). The activation time τ (Eq. 21) measures how fast the target protein becomes activated. Depicted also are the mean target activity $\bar{X}_i$ during each oscillation i (*dashed line*) and the equivalent of the numerator Q in Eq. 21 (*shadowed area*). (*B*) The ratio τ/T is plotted against the relative frequency ω using the general expression (*solid line*) given in Eq. 35, and the simplified solution (*dashed line*) in Eq. 22. Parameters: $\gamma = 0.3$, $\sigma = 2, 10$.

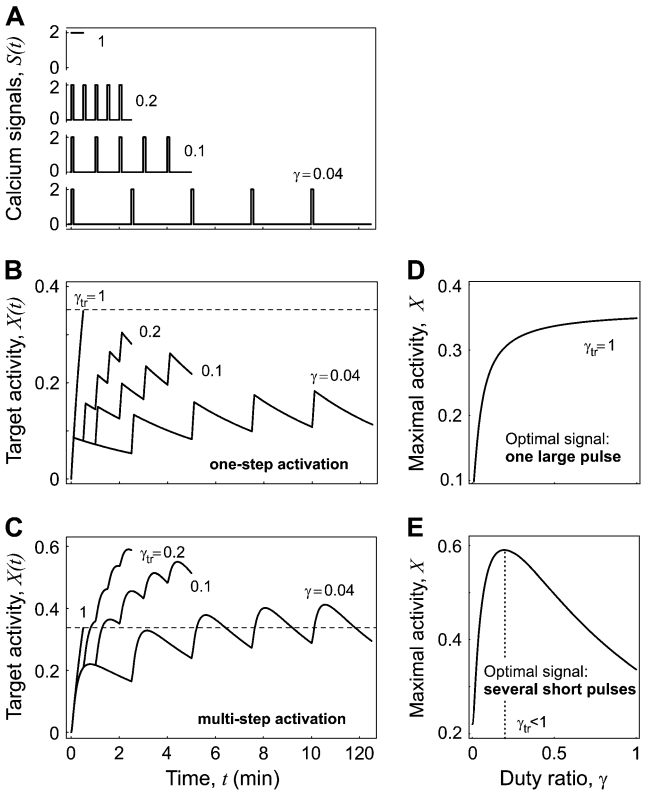

FIGURE 7 Decoding of signals with limited amount of calcium. (*A*) Transient calcium signals: Ca^{2+} stimulation is a single continuous 0.5 min pulse ($\gamma = 1$) or 5 pulses of 0.1 min durations at 0.5 min ($\gamma = 0.2$), 1 min ($\gamma = 0.1$), and 2.5 min ($\gamma = 0.04$) intervals. (*B*) When the kinase responds fast to Ca^{2+} changes (Eq. 3 holds), the optimal signal is a single continuous Ca^{2+} pulse ($\gamma_{tr} = 1$). Shown are the time-courses of the target activity X in response to the Ca^{2+} signals depicted in panel *A*. (*C*) When the kinase is slowly activated (Eqs. 1 and 2 hold), the target activity becomes maximal by applying Ca^{2+} pulses at intervals of 0.5 min ($\gamma_{tr} = 0.2$). (*D* and *E*) Mean target protein activity for the last oscillation versus the duty ratio γ. A maximal activity is obtained for the optimal duty ratio γ_{tr}. Parameters: $n = 1$, $S_0 = 2\ \mu M$, $\Delta = 0.1$ min, $m = 5$ spikes; in panels *B* and *D*, $\hat{\alpha} = 1/\text{min}$, $\beta = 0.2/\text{min}$, $K_S = 0.2\ \mu M$; in panels *C* and *E*, $\alpha_X = 1/(\mu M\ \text{min})$, $\beta_X = 0.2/\text{min}$, $\alpha_Y = 20/(\mu M\ \text{min})$, $\beta_Y = 4/\text{min}$, $Y_T = 1\ \mu M$.

Target kinetics and stimulus duration determine the optimal signal shape when calcium amount is limited

Generally the amount of Ca^{2+} elicited by cell stimulation is limited. Experiments show that in such a case the activation of Ca^{2+}-dependent transcription factors like NFAT may be optimized by releasing Ca^{2+} in the form of pulses at short-time intervals (13,16). This raises the question under which conditions Ca^{2+} release as pulses can be more effective than a single continuous signal. Which molecular features determine the optimal signal shape when Ca^{2+} amount is limited? To this end, we compared the target activity in response to Ca^{2+} signals with the same Ca^{2+} amount released either at once or as uniformly-shaped pulses at regular time intervals. The amount of calcium released is given by the total time during which $[Ca^{2+}]_c$ remains elevated (Fig. 7 *A*). The efficiency of decoding such signals can be evaluated by the maximal target activity reached during the last oscillation period.

We found that the optimal form of Ca^{2+} release is primarily determined by the rate of Ca^{2+} binding to the kinase. When Ca^{2+} binding occurs much faster than target kinetics, its activity becomes maximal by releasing Ca^{2+} at once, i.e., optimal duty ratio $\gamma_{tr} = 1$ (Fig. 7, *B* and *D*). On the contrary, when the kinase is slowly activated, the target activity is maximized by releasing Ca^{2+} in the form of repetitive short pulses, $\gamma_{tr} < 1$ (Fig. 7, *C* and *E*). While the first situation can be considered as a single-step activation (Eq. 3 holds), in the second case the target protein is activated by a two-step kinetics (Eqs. 1 and 2 hold).

To elucidate which processes control this optimal signal, we tried to simplify the full system (Eqs. 1 and 2) when Ca^{2+} binds slowly to the kinase. In such a case, a tractable approximation for the kinase activation is

$$Y(t) = \bar{Y}(1 - e^{-t/\tau}), \tag{23}$$

where $\bar{Y} = \alpha_Y S_0^n \gamma/(\alpha_Y S_0^n \gamma + \beta_Y)$is the stationary kinase activity and $\tau = (\alpha_Y S_0^n \gamma + \beta_Y)^{-1}$ its activation time. For the target protein, one obtains

$$X(t) = \bar{X}\left(1 - \frac{e^{-\beta_X t} - \beta_X \tau\, e^{-t/\tau}}{1 - \beta_X \tau}\right), \tag{24}$$

where $\bar{X} = \bar{Y}\alpha_X/\beta_X$ is the stationary target activity. The term in brackets gives the fraction of $\bar{X}$ attained after time t. Changes in the duty ratio γ exert opposite effects on these two terms. On the one hand, the kinase activity $\bar{Y}$ increases with γ leading to a higher value of $\bar{X}$. On the other hand, because the total signal duration $t_{tot} = m\Delta/\gamma$ (being m the number of spikes) decreases with γ, a lower fraction of $\bar{X}$ will be reached. The optimal signal shape arises from the tradeoff between both opposing effects.

Using Eq. 24, we determined how this optimal signal shape depends on the kinetics of the phosphorylation cycle and on the time during which $[Ca^{2+}]_c$ remains elevated. If the target protein is rapidly dephosphorylated ($\beta_X \gg 1$), the optimal signal shape will then be characterized by a rapid succession of spikes and a short total duration (Fig. 8). Conversely, for slowly responding targets, the optimal signal shape has a slow spiking frequency and lasts for longer. This optimal signal is also affected by the time $m\Delta$ during which $[Ca^{2+}]_c$ remains elevated. We found that the larger this time, the higher the optimal duty ratio will be (Fig. 8). These analytical results were confirmed by numerical simulation of the full system (compare in the *solid squares* with the *solid lines* in Fig. 8).

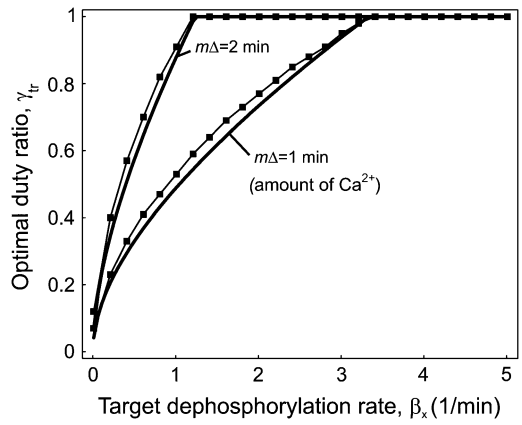

FIGURE 8 Effect of kinetic parameters on the optimal transient signal. Optimal duty ratio γ_{tr} of a transient Ca^{2+} signal as a function of the dephosphorylation rate constant β_X of the target protein. The ratio α_X/β_X is kept constant. If the target protein is rapidly inactivated ($\beta_X \gg 1$), the optimal Ca^{2+} signal is characterized by a high duty ratio. The optimal duty ratio will also increase by increasing the total duration of the Ca^{2+} spikes (*upper line*). The solid lines are calculated with the analytical approximation (Eq. 24); the solid squares are obtained after numerically solving the full system (Eqs. 2 and 3). Parameters: $n = 1$, $S_0 = 2\ \mu M$, $\Delta = 0.2$ and 0.4 min (*lower* and *upper line*, respectively), $m = 5$ spikes; $\alpha_X/\beta_X/\mu M$, $\alpha_Y = 1/(\mu M$ min), $\beta_Y = 1$/min, $Y_T = 1\ \mu M$.

In summary, when Ca^{2+} amount is limited, calcium release in the form of spikes is more effective than a single continuous release if target activation occurs in a two-step kinetics. This condition is fulfilled when Ca^{2+} binds slowly to the kinase. The optimal signal shape is determined by the amount of calcium and the kinetics of the phosphorylation cycle.

DISCUSSION

In this article, the decoding of Ca^{2+} oscillations has been theoretically analyzed in a minimal model of protein activation. Such a model comprises the activation-inactivation cycle of a target protein controlled by a Ca^{2+}-dependent kinase and the counteracting phosphatase. The mimicking of Ca^{2+} oscillations by square-shaped pulses allowed for an analytical solution of the kinetic equations. To quantify how sensitively the target protein responds to an oscillatory calcium signal, we derived expressions for the mean target activity and for the activation time. Both depend on three dimensionless quantities that govern the response of the system. Two of these dimensionless quantities (the effective activation rate and the relative oscillation frequency) combine kinetic properties of the target activation with characteristics of the Ca^{2+} signal. This fact indicates that the timescales of Ca^{2+} oscillations and target response are coupled through the decoding mechanism and should not be analyzed separately.

With our model we aimed to answer several questions concerning the decoding of Ca^{2+} oscillations:

- How does a protein respond to changes in the oscillation frequency and when does it function as a signal integrator?
- What are the advantages of having an oscillatory signal?
- Under which conditions is the system response maximized?
- To what extent do Ca^{2+} oscillations confer target specificity?

These four issues will be discussed below.

Frequency sensitivity

Although an increase in the oscillation frequency, leaving the amplitude and average unchanged, always causes an increase in the mean target activity, the magnitude of these changes depends on the inactivation rate of the target and on the duty ratio of oscillations. In case target inactivation is faster than the oscillation frequency, the target activity would simply oscillate along with the Ca^{2+} oscillation and the target does not integrate the signal. By increasing the oscillation frequency, such that Ca^{2+} oscillations are faster than target inactivation, the target protein would not fully inactivate between each Ca^{2+} oscillation and behaves as a signal integrator. In

this case, one observes a continuous increase in the target activity at each oscillation cycle. The critical point, over which the target response becomes frequency-insensitive, appears when the oscillation frequency gets in the range of the target inactivation rate. Our analysis demonstrates that true frequency decoding, at constant average Ca^{2+} signal, can indeed occur provided that Ca^{2+} spikes are narrow and the oscillation frequency is of the order of the target inactivation rate or below.

Oscillations versus constant signals

We compared the target response to a constant signal and to a sustained oscillatory signal of the same average Ca^{2+} concentration. Our analysis demonstrates that Ca^{2+} oscillations are more potent in activating the target protein than a constant signal if 1), Ca^{2+} acts cooperatively on the kinase; and 2), the Ca^{2+} sensitivity of the kinase (expressed by the dissociation constant) lies around the peak concentration of the calcium spike or above. Under these conditions, Ca^{2+} oscillations reduce the effective threshold for the target activation. Taking into account the typical values for amplitude and duty ratio of Ca^{2+} oscillations, the predicted critical affinity values lie in the range of the experimentally measured Ca^{2+} sensitivities. Furthermore, we found that target proteins are more efficiently activated by oscillatory signals at low levels of stimulation irrespective of whether the information has been encoded in the amplitude or in the frequency of oscillations. This study provides a theoretical support to the experimental findings on Ca^{2+}-dependent gene expression by Dolmetsch et al. (12) and on Ca^{2+}-dependent enzyme activation by Eshete and Fields (41), Kupzig et al. (42), and to the numerical simulations by Gall et al. (26).

Optimal signals and target specificity

We also asked, what is the calcium signal shape that best activates a particular target protein? Our analysis demonstrates the existence of an optimal shape, which is determined by the Ca^{2+} sensitivity and kinetics of target response. Thus, by varying the characteristics of Ca^{2+} oscillations, target proteins can be differentially activated. To investigate this issue, we compared two phosphorylation cycles with distinct Ca^{2+} sensitivities and (in)activation kinetics. We found that under specific conditions, Ca^{2+} oscillations can upregulate one protein and downregulate the other one and vice versa. If the cycles only differ in their (in)activation kinetics, the slowly responding protein would be always stronger-activated by Ca^{2+} oscillations than the rapidly responding protein. Such a behavior has been observed experimentally for genes regulated by the two calcium-dependent transcription factors NFAT and NFκB, where the latter factor responds slower to changes in calcium concentration (12).

Cellular responses depend not only on the frequency and amplitude of Ca^{2+} oscillations but also on the duration and number of Ca^{2+} spikes (43). Hence, we examined the specificity of target activation using time-limited Ca^{2+} oscillations. Specifically, we compared the target response when Ca^{2+} stimulation of the same total duration, i.e., the time during which calcium concentration remains elevated, is applied as either a single continuous stimulation or as pulses of short duration at distinct time intervals. Releasing Ca^{2+} at once maximizes the target response when kinase (in)activation or target (de)phosphorylation is fast compared to the duration of the Ca^{2+} transient. However, when the proteins respond slowly, the target activity becomes maximal by releasing Ca^{2+} in the form of pulses with an optimal frequency. We demonstrated analytically that this optimal oscillation frequency arises from the tradeoff between two opposing effects. On the one hand, the kinase activity increases with the oscillation frequency leading to a higher stationary target activity. On the other hand, the total signal duration decreases with the frequency so that a lower fraction of the stationary target activity will be reached. Similar conclusions were arrived at by Marhl et al. on the basis of numerical simulations (28,34).

Our theoretical analysis of target activation by transient Ca^{2+} oscillations is also consistent with the experiments of Li et al. (16) and Tomida et al. (13), who found that the nuclear localization of the transcription factor NFAT is optimized when the Ca^{2+} pulses are applied at short-time intervals. A determinant factor to achieve this effect is the temporal dissociation between Ca^{2+} signals and nuclear translocation of NFAT. Ca^{2+}-dependent dephosphorylation of NFAT proceeds faster than its nuclear translocation and rephosphorylation (44). Consequently, Ca^{2+} oscillations can induce a buildup of dephosphorylated NFAT in the cytoplasm, allowing nuclear translocation of NFAT even during the interspike interval, provided that this interval is shorter than the lifetime of dephosphorylated NFAT (13). These experiments point out to the existence of a molecular Ca^{2+} memory in the mechanism of NFAT activation, where an oscillatory input is transformed into a nearly stationary output.

Molecular sensors of calcium signals

Diverse experiments on Ca^{2+} decoding have suggested the existence of molecular sensors capable of interpreting complex temporal Ca^{2+} signals into the correct physiological response. A classic example of such decoders is the small molecule calmodulin, which activates several kinases as well as the phosphatase calcineurin (14,17). More recently, the kinase PKC (15,45) and the small GTPase Ras (46,47) have been also proposed as potential Ca^{2+} decoders. These sensors contain specialized Ca^{2+}-binding domains such as the C2 domain with a high structural diversity, allowing the binding of multiple targets with distinct Ca^{2+} sensitivities and activation kinetics. Other elements to consider are the compartmentalization and cross-interactions among signaling

molecules. So the question arises: what is the ideal processor for decoding complex Ca^{2+} signals, and what minimal features should it have?

Our study demonstrates that a system consisting of the nonlinear regulation of a target protein by a Ca^{2+}-activated kinase and the counteracting phosphatase contains the minimal features required for deciphering temporal Ca^{2+} signals. Autophosphorylation of the target protein (e.g., CaM kinase II) can be considered as a special case of this model, where the Ca^{2+}-dependent kinase is itself the target protein. Yet despite its simplicity, this minimal model is able to reproduce all features of Ca^{2+} signaling decoding that have been observed in detailed models (25,26,30). In our model, nonlinear activation of the target protein arises from the cooperative Ca^{2+} binding to the kinase. Other mechanisms that can generate nonlinear responses, such as multiple phosphorylation and feedback regulatory loops, may also be implicated in the decoding of Ca^{2+} signals and should be considered in future studies (48,49). Deciphering of complex Ca^{2+} signals presumably involves activation of multiple Ca^{2+} sensors instead of a central decoder. Complex decoding patterns such as signal integration and summation might emerge from combining single properties of the individual decoders. Therefore, it would be worth extending this approach to a system consisting of multiple Ca^{2+} decoders.

APPENDIX A: TARGET ACTIVITY AND ACTIVATION TIME

Here, we derive the formulas for the mean target activity $\bar{X}$ and the activation time τ. The linear differential equation (Eq. 3), describing the kinetics of the target protein X, can be separately solved for the spike and interspike intervals (see Eq. 5). The solution of Eq. 3 reads

$$X(t) = X_{\mathrm{i}}(\zeta) = \begin{cases} e^{-(\alpha_0+\beta)\zeta}A_{\mathrm{i}} + X_{\max}, & 0 \le \zeta < \Delta \\ e^{-\beta\zeta}B_{\mathrm{i}}, & \Delta \le \zeta \le T \end{cases}. \quad (25)$$

For simplicity, we have introduced the internal time $\zeta = t - iT$ within an oscillation cycle $\zeta \in [0,T]$. The target activity during the i^{th} cycle is denoted by $X_{\mathrm{i}}(\zeta)$. The phosphorylation rate α_0 during a Ca^{2+} spike (see Eq. 4) is given by

$$\alpha_0 = \alpha(S_0) = \hat{\alpha}\frac{(S_0/K_{\mathrm{S}})^{\mathrm{n}}}{(S_0/K_{\mathrm{S}})^{\mathrm{n}} + 1}, \quad (26)$$

and the maximal target activity is $X_{\max} = (\alpha_0)/(\alpha_0 + \beta)$. The coefficients A_{i} and B_{i} are determined from

$$X_{\mathrm{i}}(T) = X_{\mathrm{i+1}}(0) \quad \text{and} \quad X_{\mathrm{i}}(\Delta^-) = X_{\mathrm{i}}(\Delta^+), \quad (27)$$

leading to the difference equations

$$A_{\mathrm{i+1}} = e^{-(\alpha_0\Delta+\beta\mathrm{T})}A_{\mathrm{i}} - X_{\max}(1 - e^{-\beta(\mathrm{T}-\Delta)}) \text{ and}$$
$$B_{\mathrm{i}} = e^{-\alpha_0\Delta}A_{\mathrm{i}} + X_{\max}e^{\beta\Delta}. \quad (28)$$

The initial condition $X_0(0) = 0$ gives $A_0 = -X_{\max}$. Equation 28 is solved with the Ansatz $A_{\mathrm{i}} = a + be^{-\mathrm{i}(\alpha_0\Delta+\beta\mathrm{T})}$, where $e^{-\mathrm{i}(\alpha_0\Delta+\beta\mathrm{T})}$ is a solution of the homogeneous difference equation. One then obtains

$$A_{\mathrm{i}} = A_\infty\left(1 + e^{-(\mathrm{i}+1)(\beta\mathrm{T}+\alpha_0\Delta)}\frac{e^{(\alpha_0+\beta)\Delta} - 1}{1 - e^{-\beta(\mathrm{T}-\Delta)}}\right). \quad (29)$$

After a sufficiently large number of cycles ($i \to \infty$), the coefficient A_{i} approaches $A_\infty = -X_{\max}(1 - e^{-\beta(\mathrm{T}-\Delta)})/(1 - e^{-(\beta\mathrm{T}+\alpha_0\Delta)})$. Equations 28 and 29 give the second coefficient

$$B_{\mathrm{i}} = B_\infty(1 - e^{-(\mathrm{i}+1)(\beta\mathrm{T}+\alpha_0\Delta)}), \quad (30)$$

with $B_\infty = X_{\max}(e^{\beta\Delta} - e^{-\alpha_0\Delta})/(1 - e^{-(\beta\mathrm{T}+\alpha_0\Delta)})$. The dynamics of the target protein during the i^{th} cycle is then described by

$$X(t) = X_{\mathrm{i}}(\zeta) = \begin{cases} X^+(\zeta)(1 - e^{-\mathrm{i}(\beta\mathrm{T}+\alpha_0\Delta)}) + X_{\max}(1 - e^{-(\alpha_0+\beta)\zeta})e^{-\mathrm{i}(\beta\mathrm{T}+\alpha_0\Delta)}, & 0 \le \zeta < \Delta \\ X^-(\zeta)(1 - e^{-(\mathrm{i}+1)(\beta\mathrm{T}+\alpha_0\Delta)}), & \Delta \le \zeta \le T \end{cases}. \quad (31)$$

The quantities $X^+(\zeta)$ and $X^-(\zeta)$ denote the stationary target activity during a Ca^{2+} spike ($0 \le \zeta < \Delta$) and during the interspike interval ($\Delta \le \zeta \le T$), respectively,

$$X^+(\zeta) = X_{\max}\left(1 - \frac{1 - e^{-\beta(\mathrm{T}-\Delta)}}{1 - e^{-(\beta\mathrm{T}+\alpha_0\Delta)}}e^{-(\alpha_0+\beta)\zeta}\right),$$
$$X^-(\zeta) = X_{\max}\left(\frac{e^{\beta\Delta} - e^{-\alpha_0\Delta}}{1 - e^{-(\beta\mathrm{T}+\alpha_0\Delta)}}\right)e^{-\beta\zeta}. \quad (32)$$

After a sufficiently large number of oscillation cycles ($i \to \infty$), the target activity approaches $X^+(\zeta)$ and $X^-(\zeta)$.

The mean target activity $\bar{X}_{\mathrm{i}}$ during the i^{th} cycle is defined by $\bar{X}_{\mathrm{i}} = (1)/(T)\int_0^{\mathrm{T}} X_{\mathrm{i}}(\zeta)d\zeta$. Thus, integration of Eq. 31 leads to

$$\bar{X}_{\mathrm{i}} = X_{\max}\left[\frac{\Delta}{T} + \frac{\alpha_0}{\beta T(\alpha_0+\beta)}\frac{(1 - e^{-\Delta(\alpha_0+\beta)})(1 - e^{-\beta(\mathrm{T}-\Delta)})}{1 - e^{-(\beta\mathrm{T}+\alpha_0\Delta)}}\right](1 - e^{-\mathrm{i}(\beta\mathrm{T}+\alpha_0\Delta)})$$
$$+ e^{-\mathrm{i}(\beta\mathrm{T}+\alpha_0\Delta)}X_{\max}\left(\frac{\Delta}{T} + \frac{(1 - e^{-(\alpha_0+\beta)\Delta})\left(\frac{\alpha_0}{\alpha_0+\beta} - e^{-\beta(\mathrm{T}-\Delta)}\right)}{\beta T}\right). \quad (33)$$

According to Eq. 33, the mean target activity $\bar{X}$, i.e., for $i \to \infty$, reads

$$\bar{X} = X_{\max}\left[\frac{\Delta}{T} + \frac{\alpha_0}{\beta T(\alpha_0+\beta)}\frac{(1-e^{-\Delta(\alpha_0+\beta)})(1-e^{-\beta(T-\Delta)})}{1-e^{-(\beta T+\alpha_0\Delta)}}\right]. \tag{34}$$

Equation 34 is equivalent to Eq. 7, where the dimensionless parameters $\sigma = \alpha_0/\beta$, $\omega = 1/\beta T$, and $\gamma = \Delta/T$ have been introduced.

The activation time τ of the target protein, defined in Eq. 21, can be calculated using Eqs. 33 and 34. After some algebra, one obtains

$$\tau = \frac{T}{1-e^{-(\alpha_0\Delta+\beta T)}} - \frac{T[\beta\Delta + (1-e^{-(\alpha_0+\beta)\Delta})(X_{\max}-e^{-\beta(T-\Delta)})]}{\beta\Delta(1-e^{-(\alpha_0\Delta+\beta T)}) + X_{\max}(1-e^{-(\alpha_0+\beta)\Delta})(1-e^{-\beta(T-\Delta)})}. \tag{35}$$

A Taylor expansion of Eq. 35 for $T \to 0$, leaving Δ/T constant, yields

$$\tau \approx \left(\alpha_0\frac{\Delta}{T} + \beta\right)^{-1} - \frac{T-\Delta}{2}. \tag{36}$$

Equation 36 is equivalent to Eq. 22 after introducing the dimensionless parameters.

APPENDIX B: OPTIMAL CA^{2+} SIGNALS

The optimal signal shape at a given average $\bar{S}$ is the solution of $(\partial\bar{X})/(\partial\gamma) = 0$, where the amplitude S_0 has been replaced by $S_0 = \bar{S}/\gamma$. Using Eq. 13, for low-frequency oscillations ($\omega \to 0$), one obtains the maximal target response for

$$\gamma_{\max} = \bar{S}/K_S\sqrt[n]{\frac{\hat{\alpha}/\beta+1}{n-1}}. \tag{37}$$

Using Eq. 14, for high-frequency oscillations ($\omega \to \infty$), one gets

$$\gamma_{\max} = \bar{S}/K_S\sqrt[n]{\frac{1}{n-1}}. \tag{38}$$

Numerical evaluation of Eq. 7 shows that $\gamma_{\max}$ is a decreasing function of ω. Thus, Eqs. 37 and 38 give the upper and lower bound for $\gamma_{\max}$, respectively.

Oscillations and a constant signal of equal average $\bar{S}$ have the same efficiency in activating the target protein when $\bar{X} - (\hat{\alpha}\bar{S}^n)/((\beta+\hat{\alpha})\bar{S}^n + \beta K_S^n) = 0$, where the second term corresponds to the target activity obtained with the constant signal. Solving the above equation yields a critical dissociation constant $(K_S/S_0)_{crit}$. When $K_S/S_0 > (K_S/S_0)_{crit}$, oscillations are the more potent activating signals. For high frequency oscillations ($\omega \to \infty$, Eq. 14 holds), one gets

$$\left(\frac{K_S}{S_0}\right)_{crit} = \sqrt[n]{\frac{\gamma^n-\gamma^{n+1}}{\gamma-\gamma^n}}, \tag{39a}$$

and

$$\lim_{\gamma\to 1}\left(\frac{K_S}{S_0}\right)_{crit} = \frac{1}{\sqrt[n]{n-1}}. \tag{39b}$$

These formulas correspond to Eqs. 20 and 19, respectively. For low frequencies ($\omega \to 0$, Eq. 13 holds) the critical dissociation constant reads

$$\left(\frac{K_S}{S_0}\right)_{crit} = \sqrt[n]{\frac{\gamma^n-\gamma^{n+1}}{\gamma-\gamma^n}(\hat{\alpha}/\beta+1)}, \tag{40a}$$

and

$$\lim_{\gamma\to 1}\left(\frac{K_S}{S_0}\right)_{crit} = \sqrt[n]{\frac{\hat{\alpha}/\beta+1}{n-1}}. \tag{40b}$$

Since $\bar{X}(\omega\to 0) \le \bar{X} \le \bar{X}(\omega\to\infty)$, Eqs. 39 and 40 give the lower and upper bound for $(K_S/S_0)_{crit}$, respectively. Therefore, the condition for the superiority of oscillations over a constant signal is $(K_S)/(S_0) > \sqrt[n]{(\hat{\alpha}/\beta+1)/(n-1)}$. This is a more strict condition than Eq. 19, which is valid for any frequency or duty ratio.

The work was supported by the German Research Foundation (Deutschen Forschungsgemeinschaft) through the Collaborative Research Center Theoretical Biology (grant No. SFB 618) and by the German Federal Ministry of Education and Research through the Systems Biology Competence Network of Hepatocytes.

REFERENCES

1. Berridge, M. J., M. D. Bootman, and P. Lipp. 1998. Calcium—a life and death signal. *Nature*. 395:645–648.
2. Lewis, R. S. 2001. Calcium signaling mechanisms in T-lymphocytes. *Annu. Rev. Immunol.* 19:497–521.
3. Feske, S., H. Okamura, P. G. Hogan, and A. Rao. 2003. Ca^{2+}/calcineurin signaling in cells of the immune system. *Biochem. Biophys. Res. Commun.* 311:1117–1132.
4. Bito, H., and S. Takemoto-Kimura. 2003. Ca^{2+}/CREB/CBP-dependent gene regulation: a shared mechanism critical in long-term synaptic plasticity and neuronal survival. *Cell Calcium.* 34:425–430.
5. Berridge, M. J., M. D. Bootman, and H. L. Roderick. 2003. Ca^{2+} signaling: dynamics, homeostasis and remodeling. *Nat. Rev. Mol. Cell Biol.* 4:517–529.
6. Gaspers, L. D., and A. P. Thomas. 2005. Calcium signaling in liver. *Cell Calcium.* 38:329–342.
7. Schöfl, C., G. Brabant, R. D. Hesch, A. von zur Muhlen, P. H. Cobbold, and K. S. Cuthbertson. 1993. Temporal patterns of α1-receptor stimulation regulate amplitude and frequency of calcium transients. *Am. J. Physiol.* 265:C1030–C1036.
8. D'Andrea, P., F. Codazzi, D. Zacchetti, J. Meldolesi, and F. Grohovaz. 1994. Oscillations of cytosolic calcium in rat chromaffin cells: dual modulation in frequency and amplitude. *Biochem. Biophys. Res. Commun.* 205:1264–1269.
9. Dolmetsch, R. E., R. S. Lewis, C. C. Goodnow, and J. I. Healy. 1997. Differential activation of transcription factors induced by Ca^{2+} response amplitude and duration. *Nature*. 386:855–858.
10. Berridge, M. J. 2006. Calcium microdomains: organization and function. *Cell Calcium.* 40:405–412.
11. Rizzuto, R., and T. Pozzan. 2006. Microdomains of intracellular Ca^{2+}: molecular determinants and functional consequences. *Physiol. Rev.* 86: 369–408.
12. Dolmetsch, R. E., K. Xu, and R. S. Lewis. 1998. Calcium oscillations increase the efficiency and specificity of gene expression. *Nature*. 392: 933–936.
13. Tomida, T., K. Hirose, S. Takizawa, F. Shibasaki, and M. Iino. 2003. NFAT functions as a working memory of Ca^{2+} signals in decoding Ca^{2+} oscillation. *EMBO J.* 22:3825–3832.
14. Frey, N., T. A. McKinsey, and E. N. Olson. 2000. Decoding calcium signals involved in cardiac growth and function. *Nat. Med.* 6:1221–1227.
15. Reither, G., M. Schaefer, and P. Lipp. 2006. PKCα: a versatile key for decoding the cellular calcium toolkit. *J. Cell Biol.* 174:521–533.
16. Li, W., J. Llopis, M. Whitney, G. Zlokarnik, and R. Y. Tsien. 1998. Cell-permeant caged $InsP_3$ ester shows that Ca^{2+} spike frequency can optimize gene expression. *Nature*. 392:936–941.
17. De Koninck, P., and H. Schulman. 1998. Sensitivity of CaM kinase II to the frequency of Ca^{2+} oscillations. *Science*. 279:227–230.

18. Hajnoczky, G., L. D. Robb-Gaspers, M. B. Seitz, and A. P. Thomas. 1995. Decoding of cytosolic calcium oscillations in the mitochondria. *Cell.* 82:415–424.
19. Robb-Gaspers, L. D., P. Burnett, G. A. Rutter, R. M. Denton, R. Rizzuto, and A. P. Thomas. 1998. Integrating cytosolic calcium signals into mitochondrial metabolic responses. *EMBO J.* 17:4987–5000.
20. Dupont, G., G. Houart, and P. De Koninck. 2003. Sensitivity of CaM kinase II to the frequency of Ca^{2+} oscillations: a simple model. *Cell Calcium.* 34:485–497.
21. Goldbeter, A., G. Dupont, and M. J. Berridge. 1990. Minimal model for signal-induced Ca^{2+} oscillations and for their frequency encoding through protein phosphorylation. *Proc. Natl. Acad. Sci. USA.* 87:1461–1465.
22. Dupont, G., and A. Goldbeter. 1992. Protein phosphorylation driven by intracellular calcium oscillations: a kinetic analysis. *Biophys. Chem.* 42:257–270.
23. Schuster, S., M. Marhl, and T. Höfer. 2002. Modeling of simple and complex calcium oscillations. *Eur. J. Biochem.* 269:1333–1355.
24. Dupont, G., and A. Goldbeter. 1998. CaM kinase II as frequency decoder of Ca^{2+} oscillations. *Bioessays.* 20:607–610.
25. Prank, K., L. Läer, A. von zur Mühlen, G. Brabant, and C. Schöfl. 1998. Decoding of intracellular calcium spikes train. *Europhys. Lett.* 42:143–147.
26. Gall, D., E. Baus, and G. Dupont. 2000. Activation of the liver glycogen phosphorylase by Ca^{2+} oscillations: a theoretical study. *J. Theor. Biol.* 207:445–454.
27. Rozi, A., and Y. Jia. 2003. A theoretical study of effects of cytosolic Ca^{2+} oscillations on activation of glycogen phosphorylase. *Biophys. Chem.* 106:193–202.
28. Marhl, M., M. Perc, and S. Schuster. 2005. Selective regulation of cellular processes via protein cascades acting as band-pass filters for time-limited oscillations. *FEBS Lett.* 579:5461–5465.
29. Marhl, M., and V. Grubelnik. 2007. Role of cascades in converting oscillatory signals into stationary step-like responses. *Biosystems.* 87:58–67.
30. Larsen, A. Z., L. F. Olsen, and U. Kummer. 2004. On the encoding and decoding of calcium signals in hepatocytes. *Biophys. Chem.* 107:83–99.
31. Schuster, S., B. Knoke, and M. Marhl. 2005. Differential regulation of proteins by bursting calcium oscillations—a theoretical study. *Biosystems.* 81:49–63.
32. Larsen, A. Z., and U. Kummer. 2003. Information processing in calcium signal transduction. *Lect. Notes Phys.* 5623:153–178.
33. Salazar, C., A. Politi, and T. Höfer. 2004. Decoding of calcium oscillations by phosphorylation cycles. *In* Proceedings of Fourth International Workshop on Bioinformatics and Systems Biology. H. Mamitsuka, T. Smith, H. G. Holzhütter, M. Kanehisa, C. DeLisi, R. Heinrich, and S. Miyano, editors. Kyoto, Japan.
34. Marhl, M., M. Perc, and S. Schuster. 2006. A minimal model for decoding of time-limited Ca^{2+} oscillations. *Biophys. Chem.* 120:161–167.
35. Li, Y., and A. Goldbeter. 1992. Pulsatile signaling in intercellular communication. Periodic stimuli are more efficient than random or chaotic signals in a model based on receptor desensitization. *Biophys. J.* 61:161–171.
36. Zhang, M., and T. Yuang. 1998. Molecular mechanisms of calmodulin's functional versatility. *Biochem. Cell Biol.* 76:313–323.
37. Yang, J. J., A. Gawthrop, and Y. Ye. 2003. Obtaining site-specific calcium-binding affinities of calmodulin. *Protein Pept. Lett.* 10:331–345.
38. Thomas, A. P., G. S. Bird, G. Hajnoczky, L. D. Robb-Gaspers, and J. W. Putney, Jr. 1996. Spatial and temporal aspects of cellular calcium signaling. *FASEB J.* 10:1505–1507.
39. Rooney, T. A., E. J. Sass, and A. P. Thomas. 1989. Characterization of cytosolic calcium oscillations induced by phenylephrine and vasopressin in single Fura-2-loaded hepatocytes. *J. Biol. Chem.* 264:17131–17141.
40. Heinrich, R., and T. A. Rapoport. 1975. Mathematical analysis of multienzyme systems. II. Steady state and transient control. *Biosystems.* 7:130–136.
41. Eshete, F., and R. D. Fields. 2001. Spike frequency decoding and autonomous activation of Ca^{2+}-Calmodulin-dependent protein kinase II in dorsal root ganglion neurons. *J. Neurosci.* 21:6694–6705.
42. Kupzig, S., S. A. Walker, and P. J. Cullen. 2005. The frequencies of calcium oscillations are optimized for efficient calcium-mediated activation of Ras and the ERK/MAPK cascade. *Proc. Natl. Acad. Sci. USA.* 102:7577–7582.
43. Li, Y., G. X. Wang, M. Xin, H. M. Yang, X. J. Wu, and T. Li. 2004. The parameters of guard cell calcium oscillation encodes stomatal oscillation and closure in *Vicia faba*. *Plant Sci.* 166:415–421.
44. Salazar, C., and T. Höfer. 2003. Allosteric regulation of the transcription factor NFAT1 by multiple phosphorylation sites: a mathematical analysis. *J. Mol. Biol.* 327:31–45.
45. Oancea, E., and T. Meyer. 1998. Protein kinase C as a molecular machine for decoding calcium and diacylglycerol signals. *Cell.* 95:307–318.
46. Walker, S. A., P. J. Lockyer, and P. J. Cullen. 2003. The Ras binary switch: an ideal processor for decoding complex Ca^{2+} signals? *Biochem. Soc. Trans.* 31:966–969.
47. Cullen, P. J. 2006. Decoding complex Ca^{2+} signals through the modulation of Ras signaling. *Curr. Opin. Cell Biol.* 18:157–161.
48. Politi, A., L. D. Gaspers, A. P. Thomas, and T. Hofer. 2006. Models of IP_3 and Ca^{2+} oscillations: frequency encoding and identification of underlying feedbacks. *Biophys. J.* 90:3120–3133.
49. Salazar, C., and T. Höfer. 2007. Versatile regulation of multisite protein phosphorylation by the order of phosphate processing and protein-protein interactions. *FEBS J.* 274:1046–1061.
50. Cifuentes, M. E., L. Honkanen, and M. J. Rebecchi. 1993. Proteolytic fragments of phosphoinositide-specific phospholipase Cδ1. Catalytic and membrane binding properties. *J. Biol. Chem.* 268:11586–11593.
51. Rebecchi, M. J., R. Eberhardt, T. Delaney, S. Ali, and R. Bittman. 1993. Hydrolysis of short acyl chain inositol lipids by phospholipase Cδ 1. *J. Biol. Chem.* 268:1735–1741.
52. Kohout, S. C., S. Corbalan-Garcia, A. Torrecillas, J. C. Gomez-Fernandez, and J. J. Falke. 2002. C_2 domains of protein kinase C isoforms α, β, and γ: Activation parameters and calcium stoichiometries of the membrane-bound state. *Biochemistry.* 41:11411–11424.
53. Linse, S., A. Helmersson, and S. Forsen. 1991. Calcium binding to calmodulin and its globular domains. *J. Biol. Chem.* 266:8050–8054.
54. Bradshaw, J. M., Y. Kubota, T. Meyer, and H. Schulman. 2003. An ultrasensitive Ca^{2+}/calmodulin-dependent protein kinase II-protein phosphatase 1 switch facilitates specificity in postsynaptic calcium signaling. *Proc. Natl. Acad. Sci. USA.* 100:10512–10517.
55. Stemmer, P. M., and C. B. Klee. 1994. Dual calcium ion regulation of calcineurin by calmodulin and calcineurin B. *Biochemistry.* 33:6859–6866.
56. da Silva, A. C., A. H. de Araujo, O. Herzberg, J. Moult, M. Sorenson, and F. C. Reinach. 1993. Troponin-C mutants with increased calcium affinity. *Eur. J. Biochem.* 213:599–604.
57. Vinogradov, A., and A. Scarpa. 1973. The initial velocities of calcium uptake by rat liver mitochondria. *J. Biol. Chem.* 248:5527–5531.
58. Holmes, W. R. 2000. Models of calmodulin trapping and CaM kinase II activation in a dendritic spine. *J. Comput. Neurosci.* 8:65–85.